

Chapter 11

The Fate of Nitroaromatic (TNT) and Nitramine (RDX and HMX) Explosive Residues in the Presence of Pure Metal Oxides

Thomas A. Douglas,^{1,*} Marianne E. Walsh,²
Christian J. McGrath,³ Charles A. Weiss, Jr.,⁴
Ashley Marie Jaramillo,^{1,5} and Thomas P. Trainor⁵

¹U.S. Army Engineer Research and Development Center, Cold Regions Research and Engineering Laboratory, P.O. Box 35170, Fort Wainwright, Alaska 99703, USA

²U.S. Army Engineer Research and Development Center, Cold Regions Research and Engineering Laboratory, 72 Lyme Road, Hanover, New Hampshire 03755, USA

³U.S. Army Engineer Research and Development Center, Environmental Laboratory, 3909 Halls Ferry Road, Vicksburg, Mississippi 39180, USA

⁴U.S. Army Engineer Research and Development Center, Geotechnical and Structures Laboratory, 3909 Halls Ferry Road, Vicksburg, Mississippi 39180, USA

⁵University of Alaska Fairbanks, Department of Chemistry, Fairbanks, Alaska 99707, USA

*Thomas.A.Douglas@usace.army.mil

Packed beds of six different, granular, pure, metal oxide phases were loaded with explosives through controlled proximal detonation of Composition B. Composition B contains the commonly used explosives 2,4,6-trinitrotoluene (TNT), hexahydro-1,3,5-trinitro-1,3,5-triazine (RDX), and octahydro 1,3,5,7-tetranitro-1,3,5,7-tetrazocine (HMX). The metal oxides examined include magnetite (Fe₃O₄; Fe[II] and 2Fe[III]), two different hematites (Fe₂O₃; Fe[III]), manganese oxide (MnO; Mn[II]), pyrolusite (MnO₂; Mn[IV]), and aluminum oxide (Al₂O₃; Al[III]). These metal oxides were selected because of their potential to promote reductive transformation of explosive compounds. Following detonation subsamples of surficial

and bulk metal oxides were mixed in aqueous batches using ultraclean water and monitored for TNT, RDX, HMX, 2ADNT, and 4ADNT concentrations for 149 days.

Our results suggest that, even with highly controlled detonations, the explosive residues are heterogeneously loaded to the pure mineral phases. A logarithmic equation provides the best-fit description of the temporal trends in explosive analyte concentrations in the aqueous batches. RDX behaves more conservatively than TNT but does exhibit some loss from solution over time. Batches containing detonated magnetite and manganese oxide yielded the greatest loss of TNT, RDX, and HMX from solution and the highest 2ADNT and 4ADNT concentrations in the mineral material at the end of the batch experiments. These two batches also yielded the highest concentrations of the nitroso transformation products of RDX. This result suggests that reduced valence Fe and Mn metals promote explosive compound transformation, likely serving as a source of electrons for reductive transformation.

Introduction

One of the inevitable effects of military training is the deposition of explosive compounds and associated detonation residues to range soil systems. These compounds most commonly include nitroaromatics such as 2,4,6-trinitrotoluene (TNT) and nitramines like hexahydro-1,3,5-trinitro-1,3,5-triazine (RDX) and octahydro-1,3,5,7-tetranitro-1,3,5,7-tetrazocine (HMX). These explosive compounds are known toxicants (1, 2). It is well established that TNT sorbs to soil minerals (3). Further, soil organic matter (4–6), and microbes (7, 8) are associated with the transformation of TNT to 2-amino-4,6-dinitrotoluene (2ADNT) and 4-amino-2,6-dinitrotoluene (4ADNT). However, RDX and HMX are generally considered less reactive than TNT in training range soils (9–11).

Training range soils are comprised of complex and heterogeneous mixtures of crystalline and amorphous minerals and organic materials. Thus, any attempt to predict the fate and transport of explosive compounds in soils requires an understanding of the fundamental processes affecting contaminant dissolution, sorption-desorption, and transformation biogeochemically heterogeneous soil systems. If specific mineral phases are identified that promote the retention (i.e., sorption) or beneficial transformation (i.e., to less toxic compounds) of explosive compounds, it may be possible to augment impact areas, hand grenade ranges or storage areas with these materials to reduce the potential risk of off-site migration of explosive compounds.

Numerous studies guide our understanding of the interactions between explosive compounds and soil mineral phases. These include investigations of the fate of explosive compounds in clays (3, 12–15), sandy soils (9), and mixed soils (16–18). Surficial ferrous iron has been known to promote the reductive transformation of TNT (12, 13, 19, 20). However, there have been fewer studies of the role that metals (with their varied oxidation states) play in promoting explosive compound transformation (21, 22).

The aforementioned studies rely on the aqueous addition of solutions spiked with explosive compounds to load explosive compounds to soils and minerals. This is appropriate in considering the fate of dissolved explosives following their released into the environment from burn pits or legacy manufacturing or packing facilities. However, detonation processes on training ranges load substrates with residues and undetonated particles of varying mass, size, and surface area (23–26). The present investigation was designed to increase our understanding of the fate of these particular explosive compounds and their residues in the presence of pure metal oxides. Understanding the interactions of explosives with these ideal, pure mineral phases serves as a basis for expanded examination of more biogeochemically complex soil systems. Samples were exposed to detonation under controlled conditions and batch reactors were constructed by adding ultrapure water to the detonated oxide samples. Aqueous samples were extracted over a period of 149 days and analyzed for concentrations of TNT, RDX, HMX, TNT transformation products 2ADNT and 4ADNT, and RDX transformation products hexahydro-1-nitroso-3,5-dinitro-1,3,5-triazine (MNX) and hexahydro-1,3-dinitroso-5-nitro-1,3,5-triazine (DNX) over time.

Materials and Methods

Ten kilograms of six different pure metal oxide minerals were procured from suppliers (Table 1). The detonations were conducted within a 2-meter cubic detonation chamber, constructed of 8-cm thick steel that was open to air at the top. A three meter length of military Detonation Cord with an Uli knot tied in one end was placed into a paper cup containing 120 g of Composition B flakes (0.5-cm thick and less than 3 cm in length or width). The cup of Composition B was placed at the bottom of a 20-cm wide by 40-cm high by 50-cm long steel can. Five kg of each sample was loaded on top of their respective explosive charge. The sample material filled the container to height of 15 cm. The detonation cord was then initiated with a M21 shock tube initiator from location 100 meters away.

Two different types of samples were collected from each container. The surface sample was collected with a PTFE (Teflon) scoop and consisted of the upper 0.5 cm of the detonated sample. This generally consisted of small (1 to 5 mm) clumps of the original mineral particles with a dark gray to black coating. The bulk sample consisted of the remaining material in the container. Since the cup of Composition B was located below the sample the surface sample represents material that was furthest away from the explosive blast.

Table 1. Elemental and speciation information, descriptions and manufacturer's grain size information for the pure metal oxides investigated in this study.

<i>Sample</i>	<i>Metal</i>	<i>Name</i>	<i>Description</i>	<i>Source</i>	<i>Mesh size</i>	<i>Particle diameter in mm.</i>
Fe ₂ O ₃	Fe ³⁺	Hematite	Reddish powder	Fisher Scientific (Fairlawn, NJ)	<325	<0.04
Fe ₂ O ₃	Fe ³⁺	Hematite	Reddish powder	Strem Chemicals (Newburyport, MA)	<325	<0.04
Fe ₃ O ₄	Fe ²⁺ , Fe ³⁺	Magnetite	Silver granules	Greg Crocco (Albuquerque, NM)	<80	<0.18
MnO	Mn ²⁺	Manganese oxide	Green granules	Alfa Aesar (Ward Hill, MA)	<100	<0.15
MnO ₂	Mn ⁴⁺	Pyrolusite	Gray granules	Alfa Aesar (Ward Hill, MA)	<100	<0.15
Al ₂ O ₃	Al ³⁺	Aluminum oxide	White powder	Fisher Scientific (Fairlawn, NJ)	<325	<0.04

All batch slurries were prepared in duplicate. Mineral samples (3 to 15 g) were placed into an amber glass bottle containing 500 mL of 18 M Ω water leaving minimal headspace. The mass of explosive compound residues in each batch was calculated to be below the solubility of RDX (46.6 mg/L; (27)) by multiplying the acetonitrile-extractable explosive compound concentration following detonation (details below) by the mass of sample in each batch and dividing by the amount of ultrapure water added to each batch. As a consequence, we were able to estimate the maximum expected concentration of each analyte once each batch reactor was mixed. The glass bottles were capped and placed on a platform shaker and shaken continuously at 200 rpm in the dark at 25°C for five months. One (1.00) mL of each aqueous sample was collected from the batches at the following elapsed times: 1, 3, 7, 12, 23, 37, 52, 78, 100, 129, and 149 days and pipetted into a 7-mL amber glass vial with 2.0 mL deionized water and 1.0 mL acetonitrile. A total volume of only 10 mL (2%) was removed for analysis prior to termination of the batch experiments and acetonitrile extraction.

At day 149 water was decanted from the batch slurries which were placed in a convection oven at 25°C until they were dried (two days). Twenty mL of HPLC-grade acetonitrile was added to the dried mineral samples (3-15 g) and the mixture was capped and placed on a platform shaker for 24 hours. The sample vials were centrifuged at 200 rpm for 10 minutes. The acetonitrile extracts were diluted with HPLC grade acetonitrile in order to be within the calibration range of the HPLC-UV detector, and 1.00 mL of the diluted extract was mixed with 3.00 mL of deionized water into a 7-mL amber glass vial. These samples represent the acetonitrile-extractable explosive compound concentrations in the minerals at the end of the batch experiments.

Concentrations of TNT, RDX, HMX, 2ADNT, and 4ADNT were determined in the batch aqueous and acetonitrile extracted samples following SW846 Method 8330B (28). Peaks and concentrations were identified for MNX and DNX. However, the concentrations were consistently low and MNX and DNX are transient so we do not report the concentration values here. Our method could not quantify HMX transformation products. Samples were filtered through a Millex-FH PTFE (Teflon) 0.45- μ m filter unit prior to analysis. Explosive compound concentrations in aqueous solutions were determined on a Finnigan Spectra- SYSTEM P4000 (Thermo Electron Corporation, Waltham, MA) consisting of a pump and a Finnigan SpectraSYSTEM UV2000 dual wavelength UV/VIS absorbance detector at 254 nm (cell path 1 cm). A 100- μ L sample loop was used and the column was a 15 cm X 3.9-mm (4 μ m) NovaPak C8 held at 28°C and eluted with 1.4 mL/min of 15:85 isopropanol/water (v/v).

Calibration standards were prepared from 8095 Calibration Mix A (Restek Corporation Bellefonte, PA) at 1, 10, and 40 mg/mL in acetonitrile of TNT, RDX, 2ADNT, and 4ADNT. The percent relative standard deviation of the explosive compound concentration measurements was less than 2% based on numerous analyses of laboratory standards.

Results and Discussion

Following detonation the samples exhibited an irregular grayish black sheen and there was some evidence of agglomeration of detonated materials into clumped aggregates roughly 1cm in diameter and smaller (Figure 1). The lightly cemented particles are presumably attributable to the heat and pressures associated with the detonation events and the grayish coating on the mineral grains and their aggregates is most likely composed of explosive residues and/or detonation residuals (25, 26, 29, 30). This material was not present prior to detonation.

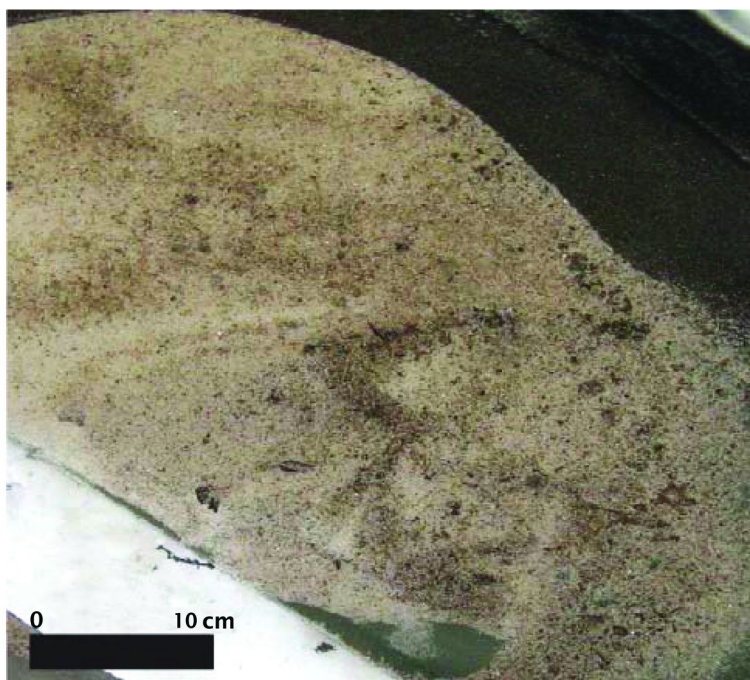


Figure 1. A photograph of the surface residue on the aluminum oxide sample following detonation.

The explosive compound concentrations measured from the batch reactor aqueous samples and the mineral sample acetonitrile extractions at day 149 are summarized in Tables 2 and 3. In all of the samples the aqueous apparent equilibrium concentration – defined here as the mean concentration of each analyte measured from the batches from day 37 onward – is greater than the maximum expected concentration. The reasons for this counterintuitive trend are unclear but some of the differences could be ascribed to the inherent heterogeneity associated with explosive compound loading to detonated samples (26). However, the “a” and “b” batches, representing duplicate batch reactors, generally yield similar results in all sample types for all analytes.

Table 2. Best fit parameters for 2,4,6-trinitrotoluene (TNT) over time from the results of the eighteen batch reactors. Aqueous-apparent equilibrium concentrations are calculated by taking the mean concentration of each analyte measured from the batches, day 37 and onward. Expected concentrations are those calculated based on combining ultraclean water with the detonated minerals. Final mineral concentrations are the acetonitrile-extractable explosive compound concentrations.

<i>Sample</i>	<i>TNT</i>					<i>2ADNT</i>		<i>4ADNT</i>	
	<i>Equation</i>	<i>r</i> ²	<i>pH at day 1</i>	<i>pH at day 149</i>	<i>Aqueous apparent equilibrium (mg/L)</i>	<i>Aqueous expected concentration at day 149 (mg/L)</i>	<i>Acetonitrile-extractable concentration at day 149 (mg/kg)</i>	<i>Acetonitrile-extractable concentration at day 149 (mg/kg)</i>	<i>Acetonitrile-extractable concentration at day 149 (mg/kg)</i>
Hematite Fisher surface a	C= -0.5 ln(t) + 24.4	0	4.3	6.9	47	20.6	52.5	0.00	0.00
Hematite Fisher surface b	C= -0.01 ln(t) + 16.5	0	4.2	6.6	28.5	20.6	95.6	0.00	0.00
Hematite Fisher bulk a	C= 1.4ln(t) + 14.2	0.05	4.6	5.8	23.3	20.5	252.7	0.00	0.00
Hematite Fisher bulk b	C= 1.1 ln(t) + 15.8	0.11	4.3	5.8	29.1	20.4	62.7	0.13	0.17
Hematite Strem surface a	C= 2.3 ln(t) + 14.0	0.35	7.9	8.8	27.7	22.1	44.4	0.14	0.12
Hematite Strem surface b	C= -0.02 ln(t) + 18.8	0	8.7	8.8	25.9	21.7	29.7	0.23	0.09
Hematite Strem bulk a	C= -2.2 ln(t) + 25.35	0.04	8.4	8.3	25.3	19.2	93.9	0.00	0.00

Continued on next page.

Table 2. (Continued). Best fit parameters for 2,4,6-trinitrotoluene (TNT) over time from the results of the eighteen batch reactors. Aqueous-apparent equilibrium concentrations are calculated by taking the mean concentration of each analyte measured from the batches, day 37 and onward. Expected concentrations are those calculated based on combining ultraclean water with the detonated minerals. Final mineral concentrations are the acetonitrile-extractable explosive compound concentrations.

<i>Sample</i>	<i>TNT</i>						<i>2ADNT</i>	<i>4ADNT</i>	
	<i>Equation</i>	<i>r</i> ²	<i>pH at day 1</i>	<i>pH at day 149</i>	<i>Aqueous apparent equilibrium (mg/L)</i>	<i>Aqueous expected concentration at day 149 (mg/L)</i>	<i>Acetonitrile-extractable concentration at day 149 (mg/kg)</i>	<i>Acetonitrile-extractable concentration at day 149 (mg/kg)</i>	<i>Acetonitrile-extractable concentration at day 149 (mg/kg)</i>
Hematite Strem bulk b	C= -1.2 ln(t) + 18.6	0.23	8.4	8.4	26.4	19.2	75.3	0.24	0.00
Magnetite sand bulk a	C= 2.0 ln(t) + 13.8	0.15	7.9	8.3	30.8	14.6	0.33	0.61	1.03
Magnetite sand bulk b	C= 2.1 ln(t) + 12.6	0.23	7.9	8.3	30.2	14.5	0.48	0.67	1.25
MnO surface a	C= -0.7 ln(t) + 16.3	0.01	7.3	7.8	25.2	19.2	68.7	1.90	1.69
MnO surface b	C= -1.7 ln(t) + 19.5	0.08	7.0	7.6	25.1	18.9	73.4	2.15	2.21
MnO bulk a	C= 0.47 ln(t) + 17.2	0.02	6.7	9.6	26	17.7	0.18	0.00	0.00
MnO bulk b	C= 1.3 ln(t) + 14.4	0.16	6.6	9.5	27.4	17.9	0.26	0.00	0.00

<i>Sample</i>	<i>TNT</i>					<i>2ADNT</i>		<i>4ADNT</i>	
	<i>Equation</i>	<i>r</i> ²	<i>pH at day 1</i>	<i>pH at day 149</i>	<i>Aqueous apparent equilibrium (mg/L)</i>	<i>Aqueous expected concentration at day 149 (mg/L)</i>	<i>Acetonitrile-extractable concentration at day 149 (mg/kg)</i>	<i>Acetonitrile-extractable concentration at day 149 (mg/kg)</i>	<i>Acetonitrile-extractable concentration at day 149 (mg/kg)</i>
MnO ₂ surface a	C= 4.1 ln(t) + 4.9	0.41	5.1	6.6	28.1	20.4	52.9	0.00	0.00
MnO ₂ surface b	C= 4.5 ln(t) + 3.2	0.23	5.1	6.8	30.3	20.4	14.3	0.00	0.00
Aluminum oxide surface a	C= 4.6 ln(t) -3.2	0.52	7.1	7.2	30.3	24.5	10.6	0.17	0.12
Aluminum oxide surface b	C= 2.5 ln(t) -1.0	0.2	7.1	7.4	26.5	24.6	4.29	0.07	0.09

Table 3. Best fit parameters for hexahydro-1,3,5-trinitro-1,3,5-triazine (RDX) over time from the results of the eighteen batch reactors. Aqueous-apparent equilibrium concentrations are calculated by taking the mean concentration of each analyte measured from the batches, day 37 and onward. Expected concentrations are those calculated based on combining ultraclean water with the detonated minerals. Final mineral concentrations are the acetonitrile-extractable explosive compound concentrations.

<i>Sample</i>	<i>RDX</i>				
	<i>Equation</i>	<i>r</i> ²	<i>Aqueous Apparent Equilibrium (mg/L)</i>	<i>Aqueous Expected concentration at day 149 (mg/L)</i>	<i>Acetonitrile-extractable concentration at day 149 (mg/kg)</i>
Hematite Fisher surface a	$C = 2.3 \ln(t) + 19.1$	0.08	41.7	31.8	257
Hematite Fisher surface b	$C = 2.1 \ln(t) + 16.0$	0.07	41.3	31.8	674
Hematite Fisher bulk a	$C = 4.0 \ln(t) + 10.1$	0.29	26.3	30.5	1287
Hematite Fisher bulk b	$C = 3.8 \ln(t) + 12.6$	0.58	32	30.3	133
Hematite Strem surface a	$C = 6.1 \ln(t) + 8.3$	0.81	39.6	33.1	195
Hematite Strem surface b	$C = 4.7 \ln(t) + 11.7$	0.43	36.2	32.5	73.6
Hematite Strem bulk a	$C = 0.3 \ln(t) + 26.4$	0	42.3	30.0	399
Hematite Strem bulk b	$C = 3.4 \ln(t) + 21.1$	0.3	30.5	30.0	381
Magnetite sand bulk a	$C = 4.6 \ln(t) + 12.8$	0.64	32.4	22.9	13.7
Magnetite sand bulk b	$C = 4.8 \ln(t) + 11.2$	0.7	32.5	22.9	14.4
MnO surface a	$C = 0.1 \ln(t) + 23.2$	0	29.1	30.0	121
MnO surface b	$C = -0.51 \ln(t) + 26.5$	0.01	29.1	29.8	147

<i>Sample</i>	<i>RDX</i>				
	<i>Equation</i>	<i>r</i> ²	<i>Aqueous Apparent Equilibrium (mg/L)</i>	<i>Aqueous Expected concentration at day 149 (mg/L)</i>	<i>Acetonitrile-extractable concentration at day 149 (mg/kg)</i>
MnO bulk a	C= 3.6 ln(t) + 15.1	0.39	32.9	29.3	0.04
MnO bulk b	C= 3.9 ln(t) + 14.7	0.49	36.3	29.5	0.13
MnO ₂ surface a	C= 6.8 ln(t) + 3.7	0.67	39.5	30.7	205
MnO ₂ surface b	C= 6.4 ln(t) + 3.2	0.45	33.8	30.7	132
Aluminum oxide surface a	C= 6.3 ln(t) -2.9	0.53	40.3	38.6	94.8
Aluminum oxide surface b	C= 5.1 ln(t) -3.3	0.4	37.8	38.9	46.5

For most of the batches the acetonitrile-extractable explosive compound concentrations recovered from the metal oxides at day 149 are greater than either the aqueous apparent equilibrium or the expected maximum concentration. This is to be expected as the batches were constructed by adding between 3 and 15 grams of detonated minerals to roughly 500 mL of ultraclean water so the final mineral acetonitrile-extractable concentrations should be greater than the apparent equilibrium or expected concentration values. However, magnetite and some of the MnO samples yielded unexpectedly low TNT, RDX, and HMX (not shown) in the acetonitrile-extractable final mineral concentrations. Aluminum oxide yielded an unexpectedly low final mineral TNT concentration. These results suggest that transformation and/or partitioning to solution have occurred in these batches.

Figures 2 and 3 include plots of TNT, RDX, HMX, and TNT transformation products 2ADNT and 4ADNT measured over time from eight of the batch reactors. All of the batches were constructed in duplicate (“a” and “b”). The differences between the “a” and “b” analyses for any given sampling day and analyte were typically within 5%. This suggests that the evolution of explosive concentration values over time in the batches is consistent among a given sample type. Only the “a” samples are presented in Figures 2 and 3 for consistency. Explosive compounds were measured each sampling day from randomly selected triplicate samples; the percent relative standard deviation for these samples was typically within 5%.

TNT has been shown to undergo transformation in a variety of aqueous reactors containing soils (16–18) and pure mineral phases (3, 10). In the magnetite sand and manganese oxide batches the TNT concentrations generally increase initially and then decrease over time. The 2ADNT and 4ADNT monoamines first begin to exceed detection limits after roughly 10 to 30 days in most batches. This is commonly around the time that TNT has reached maximum concentrations associated with dissolution and desorption processes of the explosive residues and any undetonated Composition B (23). The TNT transformation products were not present in the Composition B used to detonate the pure minerals (25) or in the initial acetonitrile extractions following detonation so their presence in the batches is most likely attributed to the reductive transformation of TNT (32, 33) during the batch experiments.

In most of the batch reactors the TNT concentrations maintain an apparent equilibrium concentration or decrease slightly around day 100 or 129. After a few weeks, 2ADNT and 4ADNT begin to be detected and in almost all of the batches at concentrations that increase and then decrease with time. This loss of 2ADNT and 4ADNT from solution could be attributed either to adsorption of these monoamines onto the metal oxide mineral surfaces or to the transformation of these compounds to phenolic derivatives (8, 25, 34). Although we did not measure the phenolic derivatives only a few of the minerals yielded detectable 2ADNT or 4ADNT in the acetonitrile-extracted samples at day 149 (Strem Fe₂O₃, magnetite sand, MnO, and Al₂O₃). This suggests that in these samples some of the 2ADNT and 4ADNT is lost from solution by sorbing onto the metal oxides. However, the acetonitrile-extractable 2ADNT and 4ADNT concentrations are 2 mg/kg or lower so they can only account for a very small fraction of the TNT

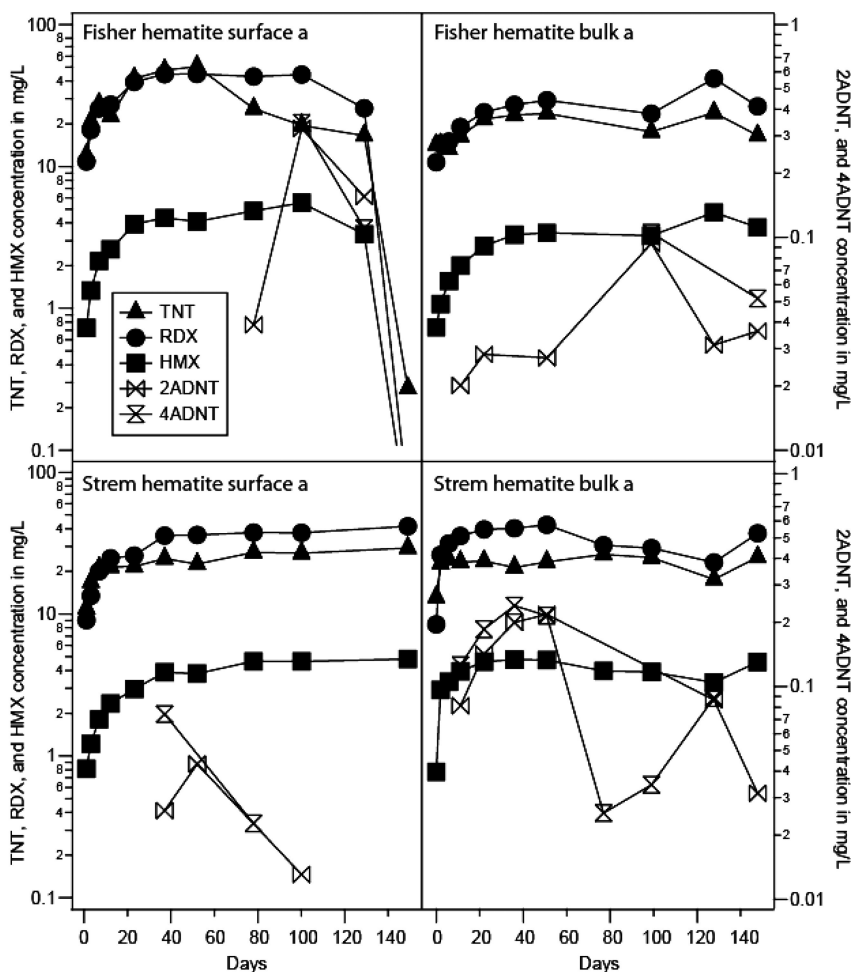


Figure 2. A plot of explosive compounds in four of the hematite batch slurries over time.

initially present as a residue on the detonated metals. In addition, the samples that yielded acetonitrile-extractable 2ADNT and 4ADNT have the lowest acetonitrile extractable TNT, RDX, and HMX concentrations so these minerals are not likely effective adsorbents for 2ADNT and 4ADNT and we can only suspect the 2ADNT and 4ADNT are transformed (8, 14, 26).

All of the batch RDX and HMX concentrations exhibit the same general trends for the first 30 days: the initial samples yield values of 5 to 15 mg/L and over the course of the next 20 to 30 days they reach an “apparent equilibrium” where adsorption-desorption and dissolution processes are approaching equilibrium (26). The explosive compound values generally remain relatively stable (primarily for RDX and HMX) for the remaining 100 days.

The acetonitrile-extractable concentrations of RDX and HMX in most of the metal oxide samples at the end of the batch experiments were greater than their

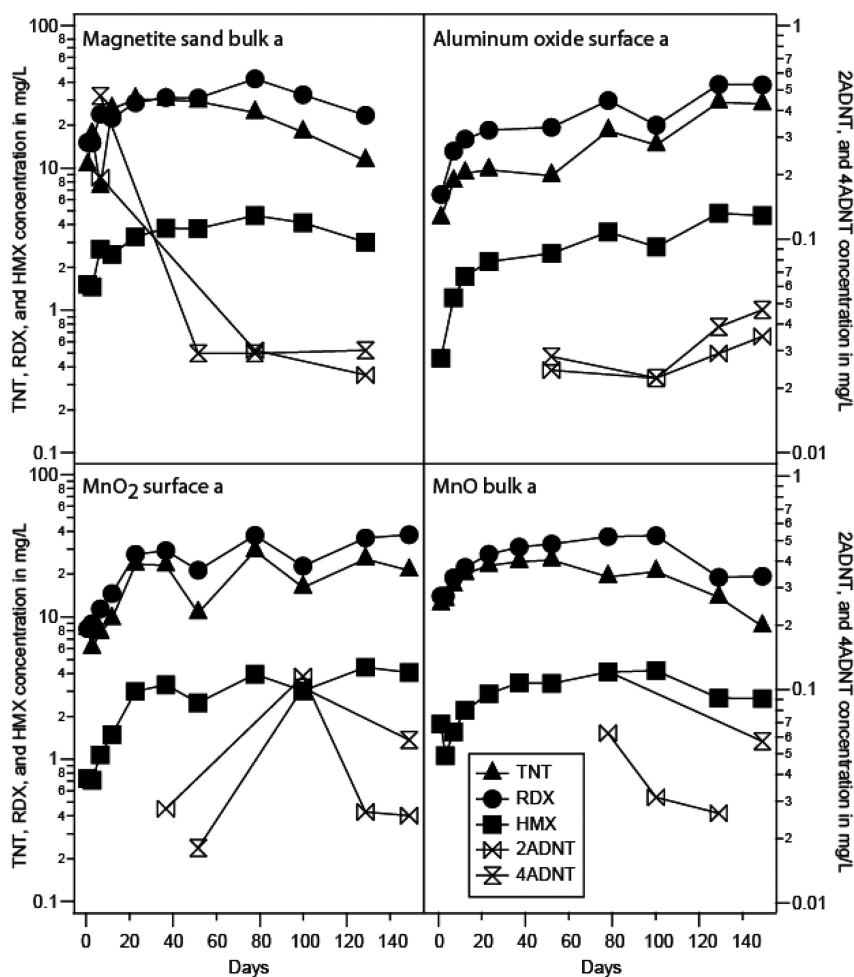


Figure 3. A plot of explosive compounds in magnetite sand, aluminum oxide, MnO and MnO₂ batch slurries over time.

concentrations in solution at any time. This implies the nitramines are readily sorbed to the metal oxides. However, RDX and HMX concentrations in the magnetite sand and manganese oxide bulk samples at day 149 were far lower than the initial RDX and HMX concentrations (compare the aqueous expected concentration at day 149 with the acetonitrile-extractable concentration at day 149 in Table 3). This might indicate these nitramines are undergoing transformation in the presence of these metal oxides. For reasons thus far undetermined, the MnO surface samples do not exhibit the same trend of lower acetonitrile-extractable concentrations at day 149 than was expected.

We identified the RDX nitroso reduction reaction products MNX and DNX in the HPLC chromatograms from all of the batch reactors. The nitroso compounds are transient intermediates in the transformation of RDX to formaldehyde, nitrous oxide gas and ammonium (30, 31). MNX concentrations were almost always

greater than DNX. MNX and DNX were detected in the initial samples of all the batches but their concentrations generally decreased to values below detection limits within 10 days. The magnetite sand and MnO top batches were the only ones for which MNX and DNX were detected in all aqueous samples. For both sample types the nitroso values peaked within 10 days and then steadily decreased to values of roughly 0.1 mg/L at day 149. The presence of these nitroso analytes in the batches signifies the transformation of RDX which was likely greatest in the magnetite sand and MnO bulk batch reactors. Our method could not quantify HMX transformation products but we speculate that the loss of HMX from solution is attributable to transformation and/or sorption.

Best fit analyses were performed for the concentration trends in RDX, HMX and TNT from the batch samples. The logarithmic fit (Tables 2 and 3) yielded the best coefficient of determination values among linear (2nd, 3rd, or 4th order), power, or exponential curve fittings. This is similar to the results from a study investigating the fate of explosive compounds in batches constructed of detonated soils (26) that provided the following equation for the logarithmic best fit of the explosive compound concentrations:

$$C=k_1\ln(t)+k_2$$

where C is the concentration in mg/L, t is the time in days, and k_1 and k_2 are fitting parameters.

It is apparent from the coefficient of determination (r^2) values for the logarithmic best fit equations (Tables 2 and 3) that TNT values are less well approximated by the logarithmic best fit equation than RDX. This can be attributed to the fact that TNT is more susceptible to transformation or adsorption than RDX or HMX (11, 14, 35–37). However, RDX does not consistently exhibit high coefficient of determination values which suggests that the dissolution and sorption-desorption processes for RDX are not at an equilibrium after 149 days, that some sorption is occurring between RDX and the metal oxides, and/or that RDX is undergoing transformation to compounds other than those measured.

In almost all of the batches the expected maximum concentrations are lower than the apparent equilibrium concentrations resulting from the logarithmic fit equations. The values are not markedly different but the reasons for this are unclear. The higher apparent equilibrium values could be explained by the limits of the logarithmic fit parameterization, by the heterogeneous loading of explosives to the detonated materials, and/or by some aspect of the desorption processes occurring in acetonitrile versus water.

The objective of this study was to determine whether pure metal oxides provide substrates that transform explosive compound residues under isothermal, aerobic, abiotic conditions in mixed batch suspensions. Metals of varying oxidation states have been shown to promote the transformation of nitroaromatic and nitramine explosive compounds, especially ferrous iron (FeII). For example, surficial structural ferrous iron on Fe²⁺-bearing clays has been found to promote the reductive transformation of TNT (13, 38–40). Iron in powdered pyrite (FeS₂; Fe[II]) and magnetite (Fe₃O₄; Fe[II and III]) has also been shown to promote the

reductive transformation of TNT, RDX, and nitroglycerin in aqueous batches (21, 22).

Conclusions

Three important conclusions can be made from this study that build on previous efforts. First, results from the batch experiments suggest that the dissolution, adsorption-desorption, and transformation processes commonly believed to occur in aqueous solutions containing explosive compounds and mineral phases appear to occur abiotically in the presence of metal oxides as well. It takes roughly 20 to 30 days to reach an apparent equilibrium and some of the explosive compounds eventually decrease in concentration. None of this is surprising but some of the mineral species evaluated here have not been evaluated previously for detonation effects or for the fate of explosive compounds in their presence.

Second, it is apparent that TNT undergoes transformation to 2ADNT and 4ADNT in the presence of all the metal oxide mineral phases regardless of their oxidation state. The mineral phases we utilized were pure phases that we believe do not contain the humic or other organic materials common in natural soils. In three of the sample types (magnetite, manganese oxide, and aluminum oxide) the 2ADNT and 4ADNT undergo transformation and exhibit minor sorption to the metal oxides.

Third, magnetite and manganese oxide are associated with the loss of RDX and HMX from solution and with the greatest TNT sorption of all the metal oxide substrates. We identified the RDX transformation products MNX and DNX in the HPLC chromatograms from all of the batches. However, the loss of RDX and HMX only occurred in the batch solutions containing magnetite and MnO. Due to their ability to transform TNT, RDX, and perhaps HMX the magnetite and MnO provide the optimal substrates to promote the transformation of TNT and the loss of nitramine compounds from solution. Based on previous research it is likely that the Fe[II] and Mn[II] present in magnetite and MnO, respectively, may serve as electron donors to promote chemical reduction transformations in explosive compounds (21, 22). Though ferrous iron minerals have been shown to provide a promising remediation component, there has been little research in using manganese as a remediation tool.

The specific surface area was not measured for any of the present oxide samples. This parameter could be a major factor in quantifying the amount of reactive substrate available to provide a medium for explosive residue transformation or sorption. However, some inferences can be made based on the particle size information. The transformation of TNT and the loss of 2ADNT and 4ADNT from solution do not appear to correlate with any particular substrate particle size. However, the two substrates that were associated with the most RDX transformation (the magnetite sand and the manganese oxide) contained the largest particle diameters (and thus the lowest specific surface areas) of our sample set. The hematite and aluminum oxide samples had much smaller particle sizes and yet these two substrates were not associated with the same degree of

RDX transformation. One reasonable next step for this investigation would be to detonate sets of pure metal oxides (and other common soil minerals) with a range of specific surface areas for each substrate and then quantify the fate of explosive residues over time.

Acknowledgments

Charles Collins, Tom Jenkins, Terry Sobecki, Susan Taylor, Dave Ringelberg, Karen Foley, Mike Reynolds, Jay Clausen, and Alan Hewitt provided insightful comments throughout the incubation and development of this project. The tests described and the resulting data presented herein, unless otherwise noted, were obtained from research conducted under the U.S. Army Environmental Quality Technology Basic Research Program by the U.S. Army Engineer Research and Development Center. The use of trade, product, or firm names in this paper is for descriptive purposes only and does not imply endorsement by the U.S. Government. Permission was granted by the Chief of Engineers to publish this information.

References

1. Rickert, D. E. E. *Toxicity of Nitroaromatic Compounds*; Hemisphere: Washington, DC, 1985.
2. Weissmahr, K. W.; Haderlein, S. B.; Schwarzenbach, R. P. *Environ. Sci. Technol.* **1997**, *31*, 240–247.
3. Larson, S.; Martin, W.; Escalon, B.; Thompson, M. *Environ. Sci. Technol.* **2008**, *42*, 786–792.
4. Tucker, W. A.; Murphy, G. J.; Arenberg, E. D. *Soil Sediment Contam.* **2002**, *11*, 809–826.
5. Eriksson, J.; Frankki, S.; Shchukarev, A.; Skyllberg, U. *Environ. Sci. Technol.* **2004**, *38*, 3074–3080.
6. Crocker, F. H.; Thompson, K. T.; Szecsody, J. E.; Freckrickson, H. L. *J. Environ. Qual.* **2005**, *34*, 2208–2216.
7. Hallas, L. E.; Alexander, M. *Appl. Environ. Microbiol.* **1983**, *45*, 1234–1241.
8. Hawari, J.; Beaudet, S.; Halasz, A.; Thiboutot, S.; Ampleman, G. *Appl. Microbiol. Biotechnol.* **2000**, *54*, 605–618.
9. Yamamoto, H.; Morley, M.; Speitel, G.; Clausen, J. *Soil Sediment Contam.: Int. J.* **2004**, *13*, 361–379.
10. Dontsova, K. M.; Hayes, C.; Pennington, J. C.; Porter, B. *J. Environ. Qual.* **2009**, *38*, 1458–1465.
11. Douglas, T. A.; Johnson, L.; Walsh, M. E.; Collins, C. *Chemosphere* **2009**, *76*, 1–8.
12. Weissmahr, K.; Haderlein, S.; Schwarzenbach, R. *Soil Sci. Soc. Am. J.* **1998**, *62*, 369–378.
13. Hofstetter, T.; Neumann, A.; Schwarzenbach, R. *Environ. Sci. Technol.* **2006**, *40*, 235–242.

14. Douglas, T. A.; Walsh, M. E.; McGrath, C. J.; Weiss, C. A. *J. Environ. Qual.* **2009**, *38* (6), 1–10.
15. Jaramillo, A. M.; Douglas, T. A.; Walsh, M. E.; Trainor, T. P. *Chemosphere* **2011**, *84* (8), 1058–1065.
16. Pennington, J. C.; Patrick, W. H., Jr. *J. Environ. Qual.* **1990**, *19*, 559–567.
17. Xue, S. K.; Selim, H. M.; Iskandar, I. K. *Soil Sci.* **1995**, *160* (5), 317–327.
18. Comfort, S. D.; Shea, P. J.; Hundal, L. S.; Li, Z.; Woodbury, B. L.; Martin, J. L.; Powers, W. L. *J. Environ. Qual.* **1995**, *24*, 1174–1182.
19. Zilberberg, I.; Pelmenschikov, A.; McGrath, C. J.; Davis, W. M.; Leszczynska, D.; Leszczynski, J. *Int. J. Mol. Sci.* **2002**, *3*, 801–813.
20. Monteil-Rivera, F.; Paquet, L.; Halasz, A.; Montgomery, M. T.; Hawari, J. *Environ. Sci. Technol.* **2005**, *39*, 9725–9731.
21. Nefso, E. K.; Burns, S. E.; McGrath, C. J. *J. Hazard. Mater.* **2005**, *B123*, 79–88.
22. Oh, S.-Y.; Chiu, P. C.; Cha, D. K. *J. Hazard. Mater.* **2008**, *158* (2–3), 652–655.
23. Ro, K.; Venugopal, A.; Adrian, D.; Constant, D.; Qaisi, K.; Valsaraj, K.; Thibodeaux, L.; Roy, D. *J. Chem. Eng. Data* **1996**, *41*, 758–761.
24. Lynch, J.; Brannon, J.; Delfino, J. *Chemosphere* **2002**, *47*, 725–734.
25. Pantea, D.; Brochu, S.; Thiboutot, S.; Ampleman, G.; Scholz, G. *Chemosphere* **2006**, *65*, 821–831.
26. Douglas, T. A.; Walsh, M. E.; McGrath, C. J.; Weiss, C. W., Jr.; Jaramillo, A. M.; Trainor, T. P. *Environ. Toxicol. Chem.* **2010**, *30* (2), 345–353.
27. Monteil-Rivera, F.; Paquet, L.; Deschamps, S.; Balakrishnan, V. K.; Beaulieu, C.; Hawari, J. *J. Chromatogr., A* **2004**, *1025*, 125–132.
28. United States Environmental Protection Agency, (USEPA). *SW846 Method 8330B USEPA Office of Solid Waste Standard Methods of Analysis Test Methods for Evaluating Solid Waste, Physical/Chemical Methods*; Office of Solid Waste: Washington, DC, 2006.
29. Hewitt, A. D.; Jenkins, T. F.; Walsh, M. E.; Walsh, M. R.; Taylor, S. *Chemosphere* **2005**, *61*, 888–894.
30. Boparai, H. K.; Comfort, S. D.; Satapanajaru, T.; Szecsody, J. E.; Grossi, P. R.; Shea, P. J. *Chemosphere* **2010**, *79*, 865–872.
31. Larese-Casanova, P.; Scherer, M. M. *Environ. Sci. Technol.* **2008**, *42*, 3975–3981.
32. Jenkins, T.; Hewitt, A.; Grant, C.; Thiboutot, S.; Ampleman, G.; Walsh, M.; Ranney, T.; Ramsey, C.; Palazzo, A.; Pennington, J. *Chemosphere* **2006**, *63*, 1280–1290.
33. Thorn, K. A.; Kennedy, K. R. *Environ. Sci. Technol.* **2002**, *36*, 3787–3796.
34. Kaplan, D. L.; Kaplan, A. M. *Appl. Environ. Microbiol.* **1982**, *44*, 757–760.
35. Haderlein, S. B.; Weissmahr, K. W.; Schwarzenbach, R. P. *Environ. Sci. Technol.* **1996**, *30*, 612–622.
36. Li, H.; Teppen, B. J.; Johnston, C. T.; Boyd, S. A. *Environ. Sci. Technol.* **2004**, *38*, 5433–5442.
37. Charles, S.; Teppen, B.; Li, H.; Laird, D.; Boyd, S. *Soil Sci. Soc. Am. J.* **2006**, *70*, 1470.

38. Hofstetter, T. B.; Schwarzenbach, R. P.; Haderlein, S. B. *Environ. Sci. Technol.* **2003**, *37*, 519–528.
39. Jaisi, D. P.; Dong, H.; Liu, C. *Geochim. Cosmochim. Acta* **2007**, *71*, 1145–1158.
40. Gregory, K. B.; Larese-Casanova, P.; Parkin, G. F.; Scherer, M. M. *Environ. Sci. Technol.* **2004**, *38*, 1408–1414.